

Chiral dynamics in $U(3)$ unitary chiral perturbation theory

Zhi-Hui Guo^{a,b}, J. A. Oller^b and J. Ruiz de Elvira^c

^a Department of Physics, Hebei Normal University, 050024 Shijiazhuang, P. R. China.

^b Departamento de Física, Universidad de Murcia, E-30071 Murcia, Spain.

^c Departamento de Física Teórica II, Universidad Complutense de Madrid, E-28040 Madrid, Spain.

November 25, 2018

Abstract

We perform a complete one-loop calculation of meson-meson scattering, and of the scalar and pseudoscalar form factors in $U(3)$ chiral perturbation theory with the inclusion of explicit resonance fields. This effective field theory takes into account the low-energy effects of the QCD $U_A(1)$ anomaly explicitly in the dynamics. The calculations are supplied by non-perturbative unitarization techniques that provide the final results for the meson-meson scattering partial waves and the scalar form factors considered. We present thorough analyses on the scattering data, resonance spectroscopy, spectral functions, Weinberg-like sum rules and semi-local duality. The last two requirements establish relations between the scalar spectrum with the pseudoscalar and vector ones, respectively. The N_C extrapolation of the various quantities is studied as well. The fulfillment of all these non-trivial aspects of the QCD dynamics by our results gives a strong support to the emerging picture for the scalar dynamics and its related spectrum.

PACS: 12.39.Fe, 11.55.Hx, 12.40.Nn, 11.15.Pg

Keywords: Chiral perturbation theory, Weinberg sum rules, semi-local duality, $1/N_C$ expansion

Chiral symmetry and $U_A(1)$ anomaly are two prominent features of QCD in the low energy sector. Chiral perturbation theory (χ PT) [1, 2, 3] that exhaustively exploits chiral symmetry as well as its spontaneous and explicit breaking to constrain the dynamics allowed, has proven as a reliable tool to analyze the QCD low energy processes involving the octet of pseudo-Goldstone bosons π , K and η . On the other hand, the $U_A(1)$ anomaly of QCD provides a natural explanation of the massive state η' [4, 5]. The consideration of a variable number of colors (N_C) in QCD is enlightening. An important finding from large N_C QCD [6] is that the $U_A(1)$ anomaly is $1/N_C$ suppressed and thus the η' meson becomes the ninth Goldstone boson at large N_C in the chiral limit [7]. This poses strong constraints on the allowed forms of the chiral operators involving the η' field, which generalizes the conventional $SU(3)$ χ PT [3] to the $U(3)$ version [4, 8, 9]. Thus $U(3)$ χ PT is a serious theory to incorporate the η' as a dynamical degree of freedom in the chiral effective Lagrangian approach and hence deserves of detailed calculations. Though the one-loop renormalization and construction of the corresponding $\mathcal{O}(p^4)$ Lagrangian are performed in Refs. [8, 9], further calculations still need to be carried out. Recently the calculation of the one-loop meson-meson scattering amplitudes was completed in Ref. [10], and the non-strangeness changing scalar and pseudoscalar form factors are calculated in the present work.

Based on the calculated scattering amplitudes and form factors from $U(3)$ χ PT, we then study semi-local duality [11, 12] between Regge theory and the hadronic degrees of freedom (h.d.f.) and construct the spectral functions to investigate the Weinberg-like spectral function sum rules [13] among the scalar and pseudoscalar correlators. The N_C evolution of the resonance poles, semi-local duality and two-point correlators are also studied. In the physical case, i.e. $N_C = 3$, the $f_0(600)$ resonance (also called σ) plays important roles for the fulfillment of both semi-local duality and the Weinberg-like spectral function sum rules. However, according to the study of Ref. [10] that employs a similar approach as the one used here, when N_C increases the $f_0(600)$ resonance evolves deeper in the complex energy plane and barely contributes at large N_C . Interestingly, we find that at large N_C the contribution from the singlet scalar resonance S_1 with a mass around 1 GeV, that is part of the $f_0(980)$ resonance at $N_C = 3$, becomes more and more important for larger values of N_C . Then, two markedly different pictures for the scalar dynamics emerge as a function of N_C . For the physical case the $f_0(600)$ is the scalar resonance mainly responsible to counterbalance the vector resonance $\rho(770)$ in semi-local duality. It also counterbalances the contributions from the octet of scalar resonances, the nonet of the pseudo-Goldstone bosons and also from the lightest multiplet of pseudoscalar resonances in the Weinberg-like spectral sum rules. However, at large N_C the remnant component (a $\bar{q}q$ -like one) of the $f_0(980)$ is responsible for the strength in the scalar dynamics. Though these two pictures differ dramatically they evolve continuously from one to the other as N_C varies. We present the discussions in more detail next.

In the perturbative calculations, we include the tree level exchanges of resonances explicitly [14], instead of considering the local chiral operators from the higher order Lagrangian [8, 9]. We then assume tacitly the saturation by resonance exchange of the (next-to-leading) chiral counterterms [14]. The relevant Lagrangian has been presented in detail in Ref. [10]. In addition we also include the exchange of pseudoscalar resonances here, which are absent in [10].

Their effects in meson-meson scattering turn out to be small, but they play a crucial role to establish the Weinberg-like spectral sum rules for the difference between the scalar-scalar (SS) and pseudoscalar-pseudoscalar (PP) correlators ($SS - PP$).

The pseudoscalar resonance Lagrangian introduced in [14] produces the mixing between the pseudoscalar resonances and the pseudo-Goldstone bosons. Nevertheless this mixing can be eliminated at the Lagrangian level through a chiral covariant redefinition of the resonance fields, which results in two local chiral operators at the $\mathcal{O}(p^4)$ level [15]. We remind that the nature of the pseudoscalar resonances is still a controversial issue and their parameters are not accurately measured yet [16]. So in order to compensate the uncertainties on the pseudoscalar resonance properties, as well as our simple parameterization here in terms of simple bare propagators in the spirit of the narrow resonance approach,¹ we include an L_8 -like operator [3].

We show the pertinent Feynman graphs for the scalar form factors of the pseudo-Goldstone pairs and the pseudoscalar form factors in the first and second rows of Fig. 1, in order. The scalar form factor of a pseudo-Goldstone boson pair PQ , $F_{PQ}^a(s)$, is defined as

$$F_{PQ}^a(s) = \frac{1}{B} \langle 0 | S^a | PQ \rangle, \quad (1)$$

while the pseudoscalar form factor of the pseudoscalar P , $H_P^a(s)$, corresponds to

$$H_P^a(s) = \frac{1}{B} \langle 0 | P^a | P \rangle. \quad (2)$$

In the equations above the scalar and pseudoscalar currents are $S^a = \bar{q} \lambda_a q$ and $P^a = i \bar{q} \gamma_5 \lambda_a q$, in order, with λ_a the Gell-Mann matrices for $a = 1, \dots, 8$ and $\lambda_0 = I_{3 \times 3} \sqrt{2/3}$ for $a = 0$. On the other hand, B is proportional to the quark condensate in the chiral limit [10]. In Fig. 1 the wavy lines correspond to either the scalar or pseudoscalar external sources, the single straight lines to the pseudo-Goldstone bosons and the double lines to the scalar (S) and pseudoscalar (P) resonances. The cross in diagram (Sd) and (Pc) indicates the coupling between the scalar resonance and the vacuum. The dot in the diagrams (Sf) and (Pd) corresponds to the vertices involving only pseudo-Goldstone bosons beyond the leading order. They can stem from many sources, such as from the local terms that originate after removing the mixing between the pseudo-Goldstone bosons and the pseudoscalar resonances. A detailed account, including explicitly all the relevant expressions, will be presented in Ref. [15].

In $U(3)$ χ PT it is necessary to resum the unitarity loops due to the large s -quark mass and the large anomaly mass. Consequently, the pseudo-Goldstone boson thresholds are much larger than the typical three-momenta in many kinematical regions, which increases the contributions from the reducible two pseudo-Goldstone boson loops [18]. Moreover, we are also interested in the resonance energy region where the unitarity upper bound in partial wave amplitudes can be easily reached, so that it does not make sense to treat unitarity perturbatively as in χ PT for these energy regions. Hence one must resum the

¹E.g. see Ref. [17] for a refined treatment of the pseudoscalar resonances as dynamically generated resonances from the interactions between the scalar resonances and the pseudo-Goldstone bosons.

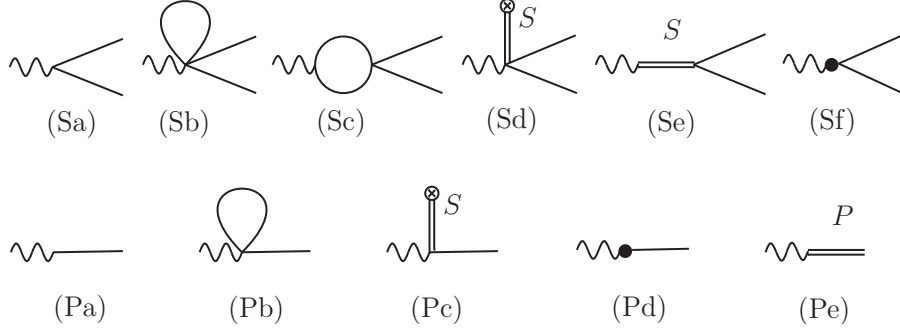


Figure 1: Feynman diagrams for the calculations of the scalar (first row) and pseudoscalar (second row) form factors. The wavy lines denote either the scalar or the pseudoscalar external source. See the text for more details.

unitary cut and we use Unitary χ PT ($U\chi$ PT) to accomplish this resummation. This approach is based on the N/D method [19] to resum the unitarity chiral loops both for the partial wave scattering amplitudes and the form factors. The application of these unitarization techniques to the form factors is discussed in Refs. [20, 21, 22]. The partial waves from $U(3)$ unitary χ PT plus the resonance exchanges at tree level were already discussed in Ref. [10], we now build the unitarized scalar form factors in a similar fashion [21]. Our master equation in matrix notation is

$$F^I(s) = [1 + N^{IJ}(s) g^{IJ}(s)]^{-1} R^I(s), \quad (3)$$

where

$$R^I(s) = F^I(s)^{(2)+\text{Res}+\text{Loop}} + T^{IJ}(s)^{(2)} g^{IJ}(s) F^I(s)^{(2)}. \quad (4)$$

In the previous equation $T^{IJ}(s)$ is a matrix whose elements are the partial wave scattering amplitudes with definite isospin I and angular momentum J . We refer to Ref. [10] for details about $T^{IJ}(s)$, $N^{IJ}(s)$ and $g^{IJ}(s)$. The quantity $F^I(s)^{(2)+\text{Res}+\text{Loop}}$ denotes the scalar form factors of the Goldstone pairs depicted in the first row of Fig. 1. The superscripts (2), Res and Loop stand for the perturbative results from the leading order, resonance contributions and chiral loops, respectively. The vector function $R^I(s)$ in Eq. (4) stems from the perturbative calculations of the form factors and it does not contain any cut singularity [20, 21].

The two-point scalar and pseudoscalar correlators, Π_{S^a} and Π_{P^a} , respectively, are defined as

$$\delta^{ab} \Pi_R(p^2) = i \int d^4x e^{ip \cdot x} \langle 0 | T[R^a(x) R^b(0)] | 0 \rangle, \quad (5)$$

with $R^a = S^a$ or P^a . After the establishment of the unitarized scalar form factors in Eq. (3), we are ready to calculate the scalar spectral function or the imaginary part of the two-point scalar correlator

$$\text{Im} \Pi_{S^a}(s) = \sum_i \rho_i(s) |F_i^a(s)|^2 \theta(s - s_i^{\text{th}}), \quad (6)$$

with $\theta(x)$ the Heaviside step function. The kinetic space factor $\rho_i(s)$ is defined as

$$\rho_i(s) = \frac{\sqrt{[s - (m_A + m_B)^2][s - (m_A - m_B)^2]}}{16\pi s}, \quad (7)$$

where m_A, m_B are the masses of the two particles in the i_{th} channel, s is the energy squared in the center of mass frame and $s_i^{\text{th}} = (m_A + m_B)^2$ denotes the threshold. We focus on the cases with $a = 0, 3$ and 8 , which conserve strangeness. The values $a = 0$ and 8 correspond to the isoscalar case $I = 0$, and there are five relevant channels: $\pi\pi$, $K\bar{K}$, $\eta\eta$, $\eta\eta'$ and $\eta'\eta'$. For $a = 3$ one has the isovector case $I = 1$ and three channels are involved: $\pi\eta$, $K\bar{K}$ and $\pi\eta'$. We adopt the isospin bases and employ the unitarity normalization as used in Ref. [10]. Another important observable that can be extracted from the scalar form factor is the quadratic pion scalar radius $\langle r^2 \rangle_S^\pi$ defined from the Taylor expansion around the origin of the pion scalar form factor as

$$F_{\pi\pi}^{\bar{u}u+\bar{d}d}(s) = F_{\pi\pi}^{\bar{u}u+\bar{d}d}(0) \left[1 + \frac{1}{6} \langle r^2 \rangle_S^\pi s + \dots \right], \quad (8)$$

with

$$m_\pi^2 F_{\pi\pi}^{\bar{u}u+\bar{d}d}(s) \equiv 2Bm \langle 0 | \bar{u}u + \bar{d}d | \pi\pi \rangle = 2Bm \left[\frac{F_{\pi\pi}^{a=8}(s)}{\sqrt{3}} + \frac{\sqrt{2} F_{\pi\pi}^{a=0}(s)}{\sqrt{3}} \right], \quad (9)$$

where m is the up or down current quark mass (isospin breaking is not considered in this work).

The pseudoscalar spectral function is related to the pseudoscalar form factors, $H_P^a(s)$, depicted in the second row of Fig. 1, by

$$\text{Im } \Pi_{P^a}(s) = \sum_i \pi \delta(s - m_{P_i}^2) |H_i^a(s)|^2, \quad (10)$$

where we do not consider multiple-particle intermediate states. In the above equation $\delta(x)$ stands for the Dirac δ function, m_{P_i} corresponds to the masses of the pseudo-Goldstone bosons or the pseudoscalar resonances with the same quantum numbers as the considered spectral function.

Another interesting object that we study is the so-called semi-local (or average) duality in scattering [11, 12]. We quantify semi-local duality in $\pi\pi$ scattering between the Regge theory and h.d.f., by employing the useful ratio between the amplitudes with well-defined I in the t -channel, as proposed in [12],

$$F_n^{II'} = \frac{\int_{\nu_1}^{\nu_{\text{max}}} \nu^{-n} \text{Im } T_t^{(I)}(\nu, t) d\nu}{\int_{\nu_1}^{\nu_{\text{max}}} \nu^{-n} \text{Im } T_t^{(I')}(\nu, t) d\nu}. \quad (11)$$

In this equation the isospin is indicated by the superscript and $\nu = \frac{s-u}{2} = \frac{2s+t-4m_\pi^2}{2}$, with s, t and u the standard Mandelstam variables. The relations between the t -channel well-defined isospin amplitudes, $T_t^{(I)}(s, t)$, and those with well-defined isospin in the s -channel, $T_s^{(I)}(s, t)$, are [11]

$$\begin{aligned} T_t^{(0)}(s, t) &= \frac{1}{3} T_s^{(0)}(s, t) + T_s^{(1)}(s, t) + \frac{5}{3} T_s^{(2)}(s, t), \\ T_t^{(1)}(s, t) &= \frac{1}{3} T_s^{(0)}(s, t) + \frac{1}{2} T_s^{(1)}(s, t) - \frac{5}{6} T_s^{(2)}(s, t), \\ T_t^{(2)}(s, t) &= \frac{1}{3} T_s^{(0)}(s, t) - \frac{1}{2} T_s^{(1)}(s, t) + \frac{1}{6} T_s^{(2)}(s, t). \end{aligned} \quad (12)$$

Since Regge exchange is highly suppressed for the exotic $I = 2$ case in the t -channel, Regge theory predicts a vanishing value for the ratios F_n^{21} and F_n^{20} . In the following we shall focus on the ratio F_n^{21} to test semi-local duality in order to make a close comparison with Ref. [12]. We study the scattering for two values of t , $t = 0$ (forward scattering) and $t = 4m_\pi^2$, in order to test the stability of the results for different small values of t compared with GeV^2 . The lower integration limit ν_1 is always set to the threshold point and we concentrate on the energy region with $\nu_{\text{max}} = 2 \text{ GeV}^2$ for the ratio in Eq. (11). To calculate in Eq. (12) the imaginary parts of the t -channel well-defined isospin amplitudes, $\text{Im } T_t^{(I)}(s, t)$, we need to know $\text{Im } T_s^{(I)}(s, t)$, which can be decomposed in the center of mass frame in a partial wave expansion as

$$\text{Im } T_s^{(I)}(\nu, t) = \sum_J (2J + 1) \text{Im } T^{IJ}(s) P_J(z_s), \quad (13)$$

with $z_s = 1 + 2t/(s - 4m_\pi^2)$, the cosine of the scattering angle, and $P_J(z_s)$ the Legendre polynomials. The partial waves $T^{IJ}(s)$ were already carefully studied in Ref. [10] within $U(3)$ unitary χ PT, and we extend the results there by including the contributions from the exchange of the pseudoscalar resonances.

We point out that all the parameters entering the form factors also appear in the unitarized scattering amplitudes and in the expressions for the masses of the pseudo-Goldstone bosons. Hence, once the unknown parameters are determined by the fit to scattering data and the pseudo-Goldstone masses, we can completely predict the form factors and spectral functions. By using the best fit in Eq. (55) of Ref.[10] for the calculation of the pion scalar form factor, a small quadratic pion scalar radius is obtained $\langle r^2 \rangle_S^\pi = 0.43 \text{ fm}^2$, which is around 30% less than the dispersive result 0.61 fm^2 in [23]. One way to improve the pion scalar radius is to increase the value of L_5 [3]. It is found in Ref. [24] that a second multiplet of scalar resonances around 2 GeV contributes around 50% of L_5 . Thus, we shall include this second scalar multiplet in our analysis and we take the values for its resonance parameters from the preferred fit Eq. (6.10) of Ref. [24]. The inclusion of this second scalar nonet and of the pseudoscalar resonance exchanges requires to perform a new fit. The resulting quality of the new fit and also the resonance spectroscopy, which will be given in detail in Ref. [15], are quite similar to the ones of Ref.[10], so we refrain from discussing them further here. But the new fit improves the pion scalar radius to $0.49_{-0.03}^{+0.01} \text{ fm}^2$, being around a 14% larger than the result from the best fit of Ref. [10].

Let us consider other interesting consequences of the new fit. As we commented previously, an important advantage of $U(3)$ χ PT, compared with the $SU(2)$ or $SU(3)$ versions, is that it incorporates the singlet η_1 that becomes the ninth Goldstone boson at large N_C in the chiral limit and thus $U(3)$ χ PT is more adequate to discuss the large N_C dynamics. The leading order N_C scaling for the various parameters in our theory was already given in [10]. For the pion decay constant F_π , we always take both the leading and sub-leading N_C terms which were calculated in Ref. [10] at the one-loop level in $U(3)$ χ PT. In addition to only including the leading N_C behavior for the remaining parameters, referred as Scenario 1, we also consider other three scenarios that include sub-leading N_C scaling for the resonance parameters. Through the fit to experimental data, we determine the values of the parameters at $N_C = 3$. By imposing short distance

constraints, the resonance parameters that then result at large N_C are already discussed in many contexts [25, 26, 27, 28]. Among these constraints, we take the one from the vector resonance sector, which should be quite reliable due to the well established $\rho(770)$ $\bar{q}q$ -like resonance at large N_C . An updated version of the constraint on G_V , a coupling describing the vertices of the $\rho(770)$ with pions, is revealed in many recent works [26, 27, 28, 10] as

$$G_V = \frac{F}{\sqrt{3}}, \quad (14)$$

with F the pion decay constant at large N_C . The extrapolation function for G_V is uniquely fixed if one considers contributions up to and including next-to-leading order in the large N_C expansion and requires G_V to take the value given by the fit at $N_C = 3$ and the result in Eq. (14) at large N_C . We present the detailed expressions in Ref. [15]. We refer the situation including the sub-leading piece for G_V as Scenario 2. In Scenario 3, on top of the setups in Scenario 2, we impose that M_ρ and M_{S_1} approach to the same value at large N_C , which can be realized naturally by tuning the corresponding parameters at the level of 16% from the values at $N_C = 3$. While in Scenario 4, we keep all the constraints from Scenario 3 and include the tensor resonances, which are the dominant contributions to the D -wave amplitudes. We follow Ref. [29] to include the tensor resonances in meson-meson scattering and also take the numerical value for the tensor coupling as determined there. The explicit calculation will be also given in detail in Ref. [15]. The characteristics of the different scenarios considered are summarized in Table 1. As proposed in Ref. [12], F_n^{21} with $n = 0, 1, 2$ and 3 are the relevant ratios in our considered energy region. We show the N_C evolution of the ratio F_n^{21} from Eq. (11) in Fig. 2 for $n = 0$ and 3. And more details for $n = 1$ and 2 will be given in Ref. [15].

	G_V	M_ρ, M_{S_1}	D -wave
Scenario 1	—	—	—
Scenario 2	✓	—	—
Scenario 3	✓	✓	—
Scenario 4	✓	✓	✓

Table 1: Description of Scenarios 1–4. In the second and third columns the symbol ✓ (—) denotes that the sub-leading N_C scaling for the corresponding parameters is (not) considered. In the last column, the symbol ✓ (—) means that we do (not) consider the contribution from the D -waves.

Notice that if the required cancellations between the $I = 0$ and $I = 1$ partial wave amplitudes in Eq. (12) did not take place for $T_t^{(2)}(s, t)$, as they are required by Regge exchange theory, the natural value for $|F_n^{21}|$ would be around 1. While if the semi-local duality is satisfied, $|F_n^{21}|$ should approach to zero. So we conclude that Scenario 3 is the best one of the four situations. The main problem in Scenario 4 is that the tensor resonances give too large contributions and overbalance the $\rho(770)$ resonance for $n = 0$. This seems to indicate that once the tensor resonances are included, heavier vector resonances are needed so as to fulfill better semi-local duality for $n = 0$. A remarkably valuable information that we can get from the study of semi-local duality is its capacity to distinguish

clearly between the different scenarios proposed and hence it provides a tight constraint on the N_C evolution of the resonance parameters. In the following we shall only focus on the N_C running within Scenario 3, since it is the one that satisfies best semi-local duality.

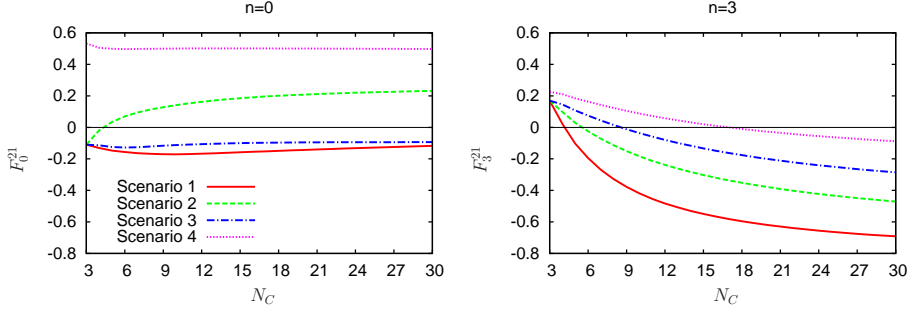


Figure 2: Evolution of $F_n^{21}(t = 4m_\pi^2)$ from $N_C = 3$ to 30 for the four scenarios considered. See the text and Table 1 for the meaning of each scenario. We verify that the ratios evaluated at $t = 0$ are similar.

Now, we study the Weinberg-like spectral sum rules in the scalar and pseudoscalar sectors, which are given by

$$\int_0^{s_0} [\text{Im } \Pi_R(s) - \text{Im } \Pi_{R'}(s)] ds + \int_{s_0}^{\infty} [\text{Im } \Pi_R(s) - \text{Im } \Pi_{R'}(s)] ds = 0, \quad (15)$$

where $R, R' = S^a$ or P^a , with $a = 0, 8, 3$. With a proper choice of s_0 , we can calculate the first integral employing the results from the present study in the non-perturbative region and use the results from the operator product expansion (OPE) to calculate the second one. According to the OPE study of Ref. [30] the different spectral functions considered here are equal in the asymptotic region in the chiral limit.² As a result the second integral in Eq. (15) is zero and to test how well the Weinberg-like spectral function sum rules hold reduces to the evaluation of the first integral in Eq. (15) in the energy region below $\sqrt{s_0}$. The relevant spectral functions $\text{Im } \Pi_R$ are calculated through Eq. (6) for the scalar case and from Eq. (10) for the pseudoscalar one. To study the dependences of the first integral in Eq. (15) with s_0 , we try three values of s_0 , namely, $s_0 = 2.5, 3.0$ and 3.5 GeV^2 and we confirm that the results are quite stable for the different values taken. In order to display the results in a more compact way, we show the value of the integral separately for each spectral function

$$W_i = 16\pi \int_0^{s_0} \text{Im } \Pi_i(s) ds, \quad i = S^8, S^0, S^3, P^0, P^8, P^3, \quad (16)$$

instead of the differences between the various correlators. We show the results for $W_i \times 3/N_C$ in Fig. 3 at the physical point and also their N_C evolution in the chiral limit. In order to study W_i in the chiral limit, we need to perform the chiral extrapolation. Though the resonance parameters are independent on the quark masses, the subtraction constants introduced through the unitarization procedure depend on them. Indeed it is shown in Ref. [31] that in the $SU(3)$

²The calculation in Ref. [30] is done up to $\mathcal{O}(\alpha_s)$ and including up to dimension 5 operators.

limit case (as in the chiral limit) all of them should be the same for any PQ pair involving the π , K and η_8 pseudoscalars. Indeed, we find that in the chiral limit there exists a reasonable region for a common value of all the subtraction constants where the values of the two-point correlators are stable and Weinberg sum rules are improved comparing with the physical situation. This region includes values similar to the ones fitted. In Fig. 3, we show the typical result in this region and normalize by the factor $3/N_C$ because W_i scales as N_C , as it is also clear from the results plotted in the figure. Focusing on the points at the chiral limit case in Fig. 3, the relative variance among the six numbers, i.e. the square root of the variance divided by their mean value [15], is found to be 10%, implying that the Weinberg-like spectral function sum rules in the $SS-SS$, $PP-PP$ and $SS-PP$ sectors hold quite accurately. The fulfillment of these sum rules even improves at large N_C and the relative variance reduces to 5% for $N_C = 30$.

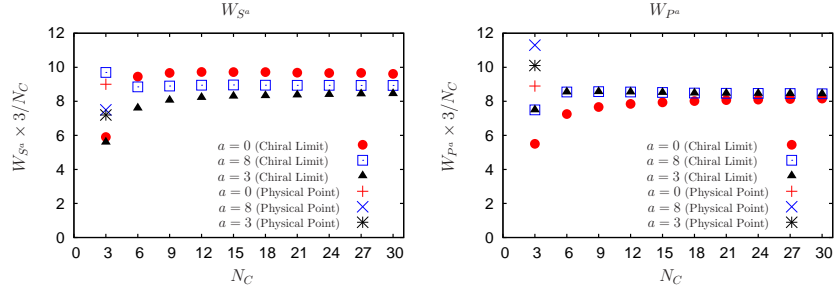


Figure 3: $W_i \times 3/N_C$ as a function of N_C within Scenario 3. All of the results are calculated by setting the upper limit of the integral in Eq. (16) to $s_0 = 3 \text{ GeV}^2$. We check that the results with $s_0 = 2.5 \text{ GeV}^2$ and $s_0 = 3.5 \text{ GeV}^2$ are quite similar.

Up to now, we have shown that our formalism can simultaneously fulfill semi-local duality between the Regge theory and h.d.f. and the Weinberg-like spectral function sum rules both for the physical case and large values of N_C . Of course this success is based on the fact that we properly take the N_C scaling for the resonance parameters dictated by the short distance constraint. It is interesting to de-construct the ratio F_n^{21} and the Weinberg-like spectral sum rules to see how different resonances contribute to them. At the physical case, we obtain the spectroscopy for various resonances, such as $f_0(600)$, $f_0(980)$, $f_0(1370)$, $a_0(980)$, $a_0(1450)$, $K_0^*(800)$ (also called κ), $K_0^*(1430)$, $\rho(770)$, $K^*(892)$ and $\phi(1020)$, and they agree quite well with their properties reported in the PDG [16]. Taking F_3^{21} as an example, we observe an interesting interplay between the $f_0(600)$ and $f_0(980)$ resonances in the N_C evolution. In Fig. 4, we show the N_C trajectories for the $f_0(600)$ and $f_0(980)$, from left to right, respectively. More details about the other resonances will be displayed elsewhere [15]. For the physical situation, both $f_0(600)$ and $\rho(770)$ give important contributions to F_3^{21} , which leads to a significant cancellation between each other, that is necessary in order to guarantee semi-local duality. While the $f_0(980)$ only plays a marginal role. But when N_C increases, the $f_0(600)$ pole as shown in Fig. 4 and in Ref. [10], blows up in the complex energy plane and does not play any significant role at large N_C . In contrast, the $\rho(770)$ resonance falls down to the real axis [32, 10],

behaving as a standard $\bar{q}q$ -like resonance at large N_C , and definitely contributes to the ratio F_3^{21} . The scalar strength to cancel the contribution from the $\rho(770)$ comes now from the $f_0(980)$ resonance, which gradually evolves to the singlet scalar $\bar{q}q$ -like S_1 when increasing N_C .

It is also worth comparing our results with those from the previous works [12, 32, 33] based on the use of the Inverse Amplitude Method [34]. The N_C trajectories shown in Fig.4, confirm again the results obtained in [32, 33] which predict a non-dominant $\bar{q}q$ behavior for the $f_0(600)$. The latter was explained in terms of different kind of resonances in Ref. [35]. Note that the $f_0(600)$ behavior in Fig. 4, moving towards lower masses and larger widths, was found in Refs. [12, 36] by varying the renormalization scale where the N_C scaling of the χ PT low energy constants applies. Let us remark that, as it happens in Ref. [12], in order to satisfy semi-local duality, we also need a $\bar{q}q$ component around 1 GeV. However, this work presents an alternative to Refs. [33, 12] because at $N_C = 3$ such a $\bar{q}q$ component would belong to the $f_0(980)$ instead to the $f_0(600)$.

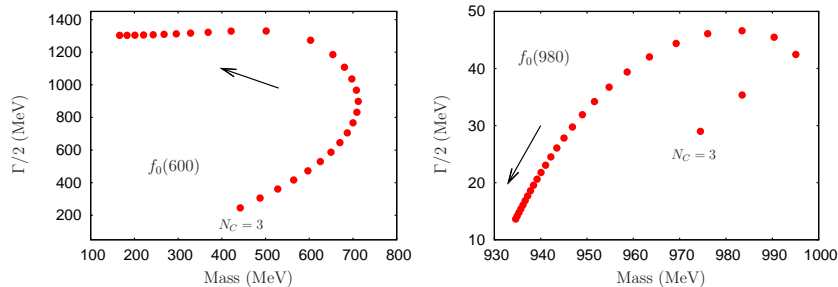


Figure 4: Pole trajectories as a function of N_C for the resonances $f_0(600)$ and $f_0(980)$. We show the results from $N_C = 3$ to 30 in one unit step.

Large cancellations are also required to satisfy the Weinberg-like spectral function sum rules. For the physical case, the singlet correlator W_{S^0} receives important contributions both from the $f_0(600)$ and $f_0(980)$. The octet W_{S^8} mainly gets contribution from the $f_0(1370)$ resonance and is also slightly contributed by the $f_0(600)$ and $f_0(980)$. For W_{S^3} , the $a_0(980)$ peak dominates its spectral function, though it receives non-negligible contributions from the $a_0(1450)$. However at large N_C , the $a_0(980)$ resonance goes deep in the complex energy plane, like the $f_0(600)$ for the isoscalar case, and hence it does not contribute to W_{S^3} any more. Instead, the $a_0(1450)$ becomes more important when increasing N_C and finally matches the contributions from the $f_0(980)$ in the singlet correlator W_{S^0} and $f_0(1370)$ in W_{S^8} , so that the Weinberg-like spectral function sum rules at large N_C are well satisfied.

Finally, we summarize briefly our work. We perform a complete one-loop calculation of the scalar and pseudoscalar form factors within $U(3)$ unitary χ PT, including the tree-level exchange of resonances. The spectral functions of the two-point correlators are constructed by using the resulting form factors (which are unitarized for the case of the scalar ones). After updating the fit in Ref. [10], which is also extended by including the explicit exchange of pseudoscalar resonances, we study the resonance spectroscopy, quadratic pion scalar radius, and

the fulfillment of semi-local duality and the Weinberg-like spectral function sum rules in the $SS-SS$, $PP-PP$ and $SS-PP$ cases, which are well satisfied. We show that it is important to take under consideration the high energy constraint for G_V , Eq. (14), in order to keep semi-local duality when varying N_C . An interesting interplay between different resonances when studying the N_C evolution of semi-local duality and the Weinberg-like spectral sum rules is revealed. In the former case the scalar and vector spectra appear tightly related and in the latter one the same can be stated for the scalar and pseudoscalar ones.

The idea to study the Weinberg sum rules in $U(3)$ χ PT was brought up by our colleague J. Prades, who unfortunately passed away. We would like to express our gratitude to his help in this subject. We also acknowledge the valuable discussions with J. R. Peláez. This work is partially funded by the grants MEC FPA2010-17806, the Fundación Séneca 11871/PI/09, the BMBF grant 06BN411, the EU-Research Infrastructure Integrating Activity “Study of Strongly Interacting Matter” (HadronPhysics2, grant No. 227431) under the Seventh Framework Program of EU and the Consolider-Ingenio 2010 Programme CPAN (CSD2007-00042). Z.H.G. also acknowledges the grants National Natural Science Foundation of China (NSFC) under contract No. 11105038, Natural Science Foundation of Hebei Province with contract No. A2011205093 and Doctor Foundation of Hebei Normal University with contract No. L2010B04.

References

- [1] S. Weinberg, *Physica A* **96** (1979) 327.
- [2] J. Gasser and H. Leutwyler, *Annals Phys.* **158** (1984) 142.
- [3] J. Gasser and H. Leutwyler, *Nucl. Phys. B* **250** (1985) 465.
- [4] P. Di Vecchia and G. Veneziano, *Nucl. Phys. B* **171** (1980) 253; C. Rosenzweig, J. Schechter and T. Trahern, *Phys. Rev. D* **21** (1980) 3388; E. Witten, *Ann. Phys.* **128** (1980) 363.
- [5] K. Karawabayashi and N. Ohta, *Nucl. Phys. B* **175** (1980) 477; *Prog. Theor. Phys.* **66** (1981) 1789.
- [6] G. 't Hooft, *Nucl. Phys. B* **72** (1974) 461; E. Witten, *Nucl. Phys. B* **160** (1979) 57.
- [7] E. Witten, *Nucl. Phys. B* **156** (1979) 269.
- [8] P. Herrera-Siklody, J. I. Latorre, P. Pascual and J. Taron *Nucl. Phys. B* **497** (1997) 345.
- [9] R. Kaiser and H. Leutwyler, *Eur. Phys. J. C* **17** (2000) 623.
- [10] Z.-H. Guo and J. A. Oller, *Phys. Rev. D* **84** (2011) 034005.
- [11] P.D.B. Collins, *An introduction to Regge theory and high energy physics* (Cambridge University Press, Cambridge, 1977).
- [12] J.R. Peláez, M.R. Pennington, J. Ruiz de Elvira and D.J. Wilson, *Phys. Rev. D* **84** (2011) 096006.

- [13] S. Weinberg, Phys. Rev. Lett. **18** (1967) 507; C. W. Bernard, A. Duncan, J. LoSecco and S. Weinberg, Phys. Rev. D **12** (1975) 792.
- [14] G. Ecker, J. Gasser, A. Pich and E. de Rafael, Nucl. Phys. B **321** (1989) 311.
- [15] Z.-H. Guo, J. A. Oller and J. Ruiz de Elvira, forthcoming.
- [16] K. Nakamura, *et al.*, J. Phys. G **37** (2010) 075021.
- [17] M. Albaladejo, J. A. Oller and L. Roca, Phys. Rev. D **82** (2010) 094019.
- [18] S. Weinberg, Nucl. Phys. B **363** (1991) 3.
- [19] J. A. Oller and E. Oset, Phys. Rev. D **60** (1999) 074023.
- [20] J. A. Oller, E. Oset and J. E. Palomar, Phys. Rev. D **63** (2001) 114009.
- [21] U. -G. Meißner and J. A. Oller, Nucl. Phys. A **679** (2001) 671.
- [22] J. A. Oller, Phys. Rev. D **71** (2005) 054030.
- [23] G. Colangelo, J. Gasser and H. Leutwyler, Nucl. Phys. B **603** (2001) 125.
- [24] M. Jamin, J. A. Oller and A. Pich, Nucl. Phys. B **622** (2002) 279.
- [25] G. Ecker, J. Gasser, H. Leutwyler, A. Pich and E. de Rafael, Phys. Lett. B **223** (1989) 425.
- [26] A. Pich, I. Rosell and J.J. Sanz-Cillero, JHEP **1102** (2011) 109.
- [27] Z.-H. Guo and P. Roig, Phys. Rev. D **82** (2010) 113016.
- [28] Z.-H. Guo, J. J. Sanz-Cillero and H.-Q. Zheng, JHEP **06** (2007) 030.
- [29] G. Ecker and C. Zauner, Eur. Phys. J. C **52** (2007) 315.
- [30] M. Jamin and M. Munz, Z. Phys. C **60** (1993) 569.
- [31] D. Jido, J. A. Oller, E. Oset, A. Ramos and U. G. Meissner, Nucl. Phys. A **725** (2003) 181.
- [32] J. R. Peláez, Phys. Rev. Lett. **92** (2004) 102001.
- [33] J. R. Peláez, G. Rios, Phys. Rev. Lett. **97** (2006) 242002.
- [34] A. Dobado, M. J. Herrero and T. N. Truong, Phys. Lett. B **235** (1990) 134; A. Dobado and J. R. Peláez, Phys. Rev. D **56** (1997) 3057; J. A. Oller, E. Oset and J. R. Peláez, Phys. Rev. Lett. **80** (1998) 3452; Phys. Rev. D **59** (1999) 074001; (E)-*ibid* D **60** (1999) 099906; (E)-*ibid* D **75** (2007) 099903.
- [35] F. J. Llanes-Estrada, J. R. Pelaez and J. Ruiz de Elvira, Nucl. Phys. Proc. Suppl. **207-208** (2010) 169.
- [36] J. R. Pelaez, hep-ph/0509284.